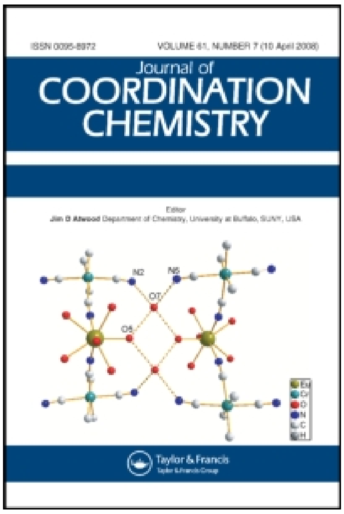

Journal of Coordination Chemistry
Publication details, including instructions for authors and subscription information:
http://www.informaworld.com/smpp/title~content=t713455674

A trinuclear Ni(II) cluster with two significantly different configurations in the solid state

Wen-Kui Dong[a]; Jin-Gui Duan[a]
[a] School of Chemical and Biological Engineering, Lanzhou Jiaotong University, Lanzhou, Gansu, P.R. China

To cite this Article Dong, Wen-Kui and Duan, Jin-Gui(2008) 'A trinuclear Ni(II) cluster with two significantly different configurations in the solid state', Journal of Coordination Chemistry, 61: 5, 781 — 788, First published on: 27 August 2007 (iFirst)

To link to this Article: DOI: 10.1080/00958970701376291

URL: http://dx.doi.org/10.1080/00958970701376291

Journal of Coordination Chemistry
Vol. 61, No. 5, 10 March 2008, 781–788

A trinuclear Ni(II) cluster with two significantly different configurations in the solid state

WEN-KUI DONG* and JIN-GUI DUAN

School of Chemical and Biological Engineering, Lanzhou Jiaotong University,
Lanzhou, Gansu, 730070, P.R. China

(*Received 21 December 2006; revised 4 March 2007; in final form 8 March 2007*)

A chelating bisoxime ligand, 2,2′-[(1,3-propylene)dioxybis(nitrilomethylidyne)]dinaphthol (H_2L), and its corresponding Ni(II) cluster $\{[NiL(H_2O)]_2(OAc)_2Ni\} \cdot 0.5MeOH \cdot 0.5CH_3CN \cdot H_2O$ (**1**) have been synthesized and characterized by elemental analyses, TG-DTA, IR, ^{1}H NMR and X-ray diffraction methods. The Ni(II) cluster is monoclinic, space group $P2(1)/c$ with cell dimensions $a = 9.400(2)$, $b = 24.530(4)$, $c = 25.350(3)$ Å and $\beta = 92.823(3)^\circ$. In the Ni(II) cluster, there are two ligand moieties (which provide N_2O_2 donors), two acetate ions and two water molecules, which result in three slightly distorted octahedral geometries around the Ni(II) ions.

Keywords: 2,2′-[(1,3-propylene)dioxybis(nitrilomethylidyne)]dinaphthol; μ-phenoxo; μ-acetato; Nickel(II) cluster; Crystal structure

1. Introduction

Schiff-base compounds constitute an important class of ligands which have been extensively investigated in coordination chemistry mainly due to their facile synthesis and easily tunable steric, electronic, and catalytic properties. They are also useful in constructing supramolecular structures [1, 2]. Cobalt(II) and manganese(II) complexes with tetradentate Schiff-base ligands which coordinate through N_2O_2 donor atoms have been studied as oxygen-carriers and also as catalysts for water splitting [3, 4]. Schiff-base complexes are also known for biological activities such as photosynthesis and transport of oxygen in mammalian and other respiratory systems [5]. Complexes of nickel with a wide variety of Schiff bases having donor atoms such as N_2O_2, N_4 and N_2S_2 around the metal have been used as catalysts for carbonylation, hydrogenation, hydroformylation and epoxidation reactions [6–11]. We have synthesized a ligand that resists C=N exchange reaction, 2,2′-[(1,3-propylene)dioxybis(nitrilomethylidyne)] dinaphthol (H_2L) and its corresponding Ni(II) cluster. The unit cell contains two crystallographically independent but chemically identical trinuclear clusters (molecules 1 and 2, see figure 4) with three octahedral geometries in a single molecule.

---

*Corresponding author. Email: dongwk@mail.lzjtu.cn

Journal of Coordination Chemistry
ISSN 0095-8972 print/ISSN 1029-0389 online © 2008 Taylor & Francis
DOI: 10.1080/00958970701376291

2. Experimental

2.1. *Reagents and physical measurements*

2-Hydroxy-1-naphthaldehyde from Aldrich was used without further purification. 1,3-dibromopropane was dried and redistilled before using. The other reagents and solvents were analytical grade from Tianjin Chemical Reagent Factory. Elemental analysis for Ni was obtained on an IRIS ER/S · WP-1 ICP atomic emission spectrometer. C, H and N analyses were carried out with a GmbH VariuoEL V3.00 automatic elemental analyzer. IR spectra in the range 500–4000 cm^{-1} were recorded on a VERTEX70 FT-IR spectrophotometer using KBr pellets. TG-DTA analysis was carried out at a heating rate of 3°C min^{-1} on a ZRY-1P thermoanalyzer. 1H NMR spectra were recorded on a Mercury-400BB spectrometer. X-ray single crystal structures were determined on a Bruker Smart APEX CCD area detector. Melting points were measured by the use of $a \times 10$ microscopic melting point apparatus made in Beijing Taike Instrument Limited Company, and the thermometer was uncorrected.

2.2. *Preparation of H_2L*

2,2′-[(1,3-propylene)dioxybis(nitrilomethylidyne)]dinaphthol (H_2L) was synthesized according to a method reported earlier [12–14]. Yield, 49%, m.p. 160–161°C, Anal. Calcd for $C_{25}H_{22}N_2O_4$: C, 72.45; H, 5.35; N, 6.76; Found: C, 72.37; H, 5.39; N, 6.82; ^{1}H NMR (400 MHz, $CDCl_3$) σ 1.57 (s, 2H), 2.27 (t, $J = 6.2$ Hz, 2H), 4.43 (t, $J = 6.2$ Hz, 4H), 7.20 (d, $J = 8.0$ Hz, 2H), 7.37 (t, $J = 7.4$ Hz, 2H), 7.51 (t, $J = 8.4$ Hz, 2H), 7.78 (d, $J = 8.8$ Hz, 2H), 7.96 (d, $J = 8.8$ Hz, 2H), 9.14 (s, 2H), 10.97 (s, 2H).

Crystals of H_2L suitable for X-ray crystal analysis were grown from ethanol solution by slow evaporation of the solvent at room temperature.

2.3. *Preparation of $\{[NiL(H_2O)]_2(OAc)_2Ni\} \cdot MeOH \cdot H_2O$ and crystal 1*

A solution of Ni(II) acetate tetrahydrate (24.89 mg, 0.10 mmol) in methanol (12 mL) was added dropwise to a solution of H_2L (41.03 mg, 0.10 mmol) in acetonitrile/chloroform (4 : 1) (15 mL) at room temperature. The color turned pale-green immediately, and stirring was continued for 8 h at room temperature whereupon a green precipitate formed. The solid was collected by filtration and the mother liquor was set aside. The resulting solid was then washed with methanol : diethylether (1 : 2) and diethylether. Yield 0.0173 g, 43%. Anal. Calcd for $\{[NiL(H_2O)]_2(OAc)_2Ni\} \cdot MeOH \cdot H_2O$ (%): C, 54.81; H, 4.68; N, 4.65; Ni, 14.61. Found: C, 54.93; H, 4.65; N, 4.74; Ni, 14.43.

Crystals suitable for X-ray analysis were obtained directly from the above mother liquor over one week as the solution slowly evaporated; these were found to be $\{[NiL(H_2O)]_2(OAc)_2Ni\} \cdot 0.5MeOH \cdot 0.5CH_3CN \cdot H_2O$ (**1**).

2.4. *IR spectra of H_2L and $\{[NiL(H_2O)]_2(OAc)_2Ni\} \cdot MeOH \cdot H_2O$*

IR spectra of H_2L and $\{[NiL(H_2O)]_2(OAc)_2Ni\} \cdot MeOH \cdot H_2O$ are shown in figure 1. The bands due to $\nu_{C=N}$ and $\nu_{Ar\text{–}O}$ of the cluster were lowered by 4 and 47 cm^{-1} respectively, as compared to H_2L values ($\nu_{C=N}$ and $\nu_{Ar\text{–}O}$ at 1604 and 1238 cm^{-1}

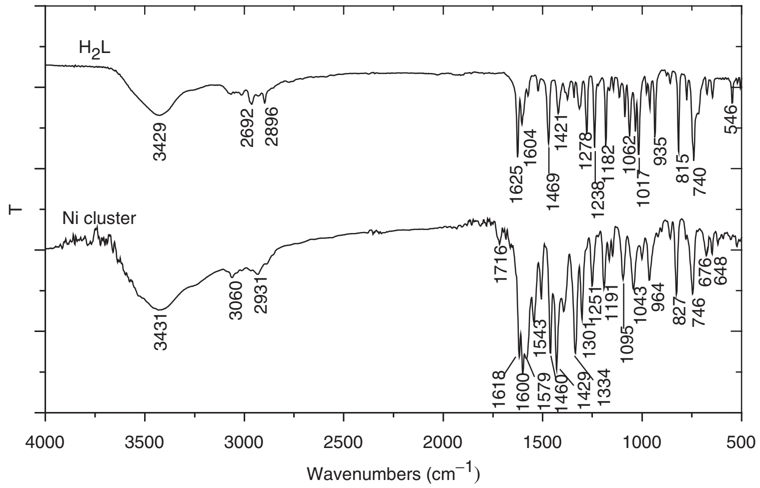

Figure 1. Infrared spectra of H_2L and $\{[NiL(H_2O)]_2(OAc)_2Ni\} \cdot MeOH \cdot H_2O$.

respectively), providing evidence for coordination of H_2L with Ni(II). A bending vibration of naphtholic alcohol in H_2L at 1278 cm^{-1} disappears in the cluster, indicating the oxygen in naphtholic alcohol of the cluster has been deprotonated and coordinated to the metals. In addition, the infrared spectrum of the Ni(II) cluster shows the expected absorptions due to the stretching, bending and wagging modes of water at 3431, 1618, and ca 522 cm^{-1}, respectively, indicating the presence of coordinated water molecules [15].

2.5. *TG-DTA of $\{[NiL(H_2O)]_2(OAc)_2Ni\} \cdot MeOH \cdot H_2O$*

Thermal decomposition of $\{[NiL(H_2O)]_2(OAc)_2Ni\} \cdot MeOH \cdot H_2O$ can be divided into four stages. The first stage is 52° to 89° with weight loss of 4.4% (4.2% calculated for the loss of crystallizing methanol and water molecules). The second stage is 104° to 120° with weight loss of 3.1%, which corresponds to the loss of two water molecules coordinated to Ni. The third stage degradation temperature is in the range 232° to 248° with mass loss of 19.2%, in which two acetate ions are removed with theoretical loss of 19.6%. The solid remains stable up to 355° and the fourth weight loss starts at around 358° to 361° with decomposition of the compound. The TG curve shows 62.5% weight loss at 362° indicating complete removal of organic material. The main product was NiO with a residual value of 37.5% (theoretical residual value was 37.2%).

2.6. *X-ray crystallography of H_2L and (1)*

The single crystals of H_2L and **1** with approximate dimensions of $0.08 \times 0.48 \times 0.70\,mm^3$ and $0.45 \times 0.23 \times 0.19\,mm^3$ were placed on a Bruker Smart Apex CCD area detector. Data were collected using graphite monochromated Mo-Kα radiation ($\lambda = 0.71073$ Å) at 298(2) and 293(2) K, respectively. The structures were solved by using SHELXL-97 and Fourier difference techniques, and refined by full-matrix least-squares on F^2. Details of the data collection and refinements are given in table 1. All hydrogen atoms were added theoretically.

3. Results and discussion

3.1. *The crystal structure of H_2L*

The crystal structure of H_2L was determined by X-ray crystallography (figure 2, figure 3, and table 2). The molecule adopts an extended conformation where the two naphthaldoxime moieties are apart. The oxime groups and naphtholic alcohols have anti-conformation, and there is an intramolecular hydrogen bond, O(2)–H(2)···N(1) (2.566(7) Å).

3.2. *The crystal structure of (1)*

X-ray crystallographic analysis of **1** reveals a symmetric trinuclear structure. The Ni(II) cluster crystallizes in the monoclinic system, space group *P*2(1)/*c*, and the unit cell contains two crystallographically independent but chemically identical trinuclear clusters (molecules 1 and 2, figure 4) consisting of two ligand units, three nickel(II) atoms, two acetates, and two water molecules as expected from the analytical data. Each inner nickel is six-coordinate. Ni(1) is located in the N_2O_2 of the ligand. One oxygen atom (O(7)) from water and one oxygen atom (O(5)) from the bridging acetate ion are also coordinated to Ni(1); Ni(1) is a slightly distorted octahedral geometry. The central nickel (Ni(2)) coordination sphere is completed by four μ-phenoxo oxygen

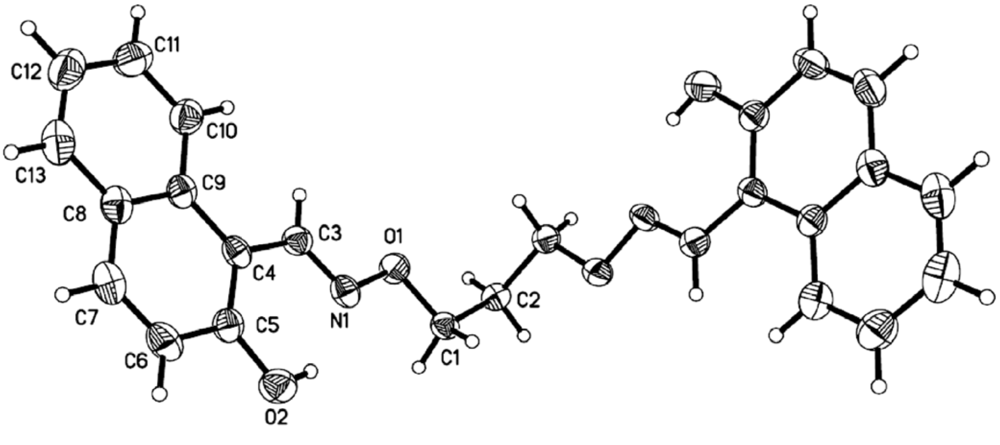

Figure 2. The structure of H_2L with the atom numbering. Displacement ellipsoids for non-H atoms are drawn at the 30% probability level.

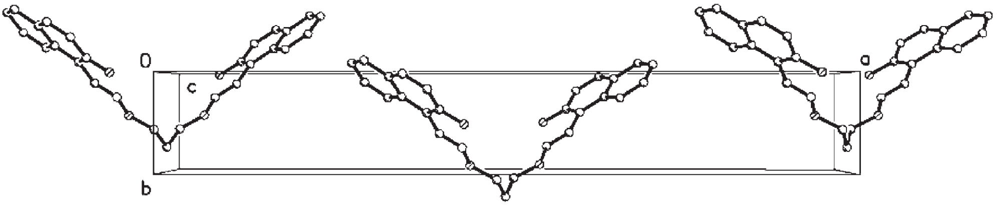

Figure 3. Packing diagram of H_2L along *c*-axis. H atoms are omitted for clarity.

Table 1. Crystal data and structure refinement for H_2L and **1**.

	H_2L	**1**
Empirical formula	$C_{25}H_{22}N_2O_4$	$C_{55.50}H_{55.50}N_{4.50}Ni_3O_{15.50}$
Formula weight	414.45	1209.67
Temperature (K)	298(2)	293(2)
Wavelength (Å)	0.71073	0.71073
Crystal system, space group	Monoclinic, $C2$	Monoclinic, $P2(1)/c$
Unit cell dimensions (Å, °)		
a	31.850(3)	9.400(2)
b	4.666(2)	24.530(4)
c	6.899(3)	25.350(3)
α	90	90
β	91.396	92.823(3)°
γ	90	90
Volume (Å^3)	1025.0(6)	5838.2(18)
Z, Calculated density (Mg m^3)	2, 1.343	4, 1.376
Absorption coefficient (mm^{-1})	0.092	1.026
$F(000)$	436	2512
Crystal size (mm^3)	$0.70 \times 0.48 \times 0.08$	$0.45 \times 0.23 \times 0.19$
θ range for data collection (°)	1.28 to 24.99	1.66–25.01
Limiting indices	$-37 \le h \le 37$, $-4 \le k \le 5$, $-6 \le l \le 8$	$-11 \le h \le 11$, $-29 \le k \le 29$, $-22 \le l \le 30$
Reflections collected/unique	2639/1027 [$R_{\text{int}} = 0.1010$]	27524/9509 [$R_{\text{int}} = 0.0895$]
Completeness to θ	99.9% ($\theta = 25.02°$)	92.4% ($\theta = 25.01°$)
Absorption correction	Semi-empirical from equivalents	Semi-empirical from equivalents
Max. and min. transmission	0.9927 and 0.9385	0.8289 and 0.6553
Refinement method	Full-matrix least-squares on F^2	Full-matrix least-squares on F^2
Data/restraints/parameters	1027/1/141	9509/27/742
Goodness-of-fit on F^2	0.987	1.104
Final R indices [$I > 2\sigma(I)$]	$R_1 = 0.0490$, $wR_2 = 0.0825$	$R_1 = 0.0939$, $wR_2 = 0.1890$
R indices (all data)	$R_1 = 0.0979$, $wR_2 = 0.0970$	$R_1 = 0.1496$, $wR_2 = 0.2161$
Largest diff. peak and hole (e Å^{-3})	0.156 and −0.171	1.052 and −0.426

Table 2. Selected bond distances (Å) and bond angles (°) for H_2L.

N(1)–C(3)	1.267(5)	C(3)–C(4)	1.450(5)	C(8)–C(9)	1.408(6)
N(1)–O(1)	1.398(4)	C(4)–C(5)	1.378(5)	C(8)–C(13)	1.410(6)
O(1)–C(1)	1.433(4)	C(4)–C(9)	1.424(5)	C(9)–C(10)	1.402(5)
O(2)–C(5)	1.354(5)	C(5)–C(6)	1.409(6)	C(10)–C(11)	1.354(6)
C(1)–C(2)	1.517(6)	C(6)–C(7)	1.335(6)	C(11)–C(12)	1.399(6)
C(2)–C(1)#1	1.517(6)	C(7)–C(8)	1.400(5)	C(12)–C(13)	1.355(6)
C(3)–N(1)–O(1)	112.8(4)	O(2)–C(5)–C(4)	123.3(5)	C(10)–C(9)–C(8)	117.2(4)
N(1)–O(1)–C(1)	108.8(3)	O(2)–C(5)–C(6)	115.5(4)	C(10)–C(9)–C(4)	123.4(5)
O(1)–C(1)–C(2)	107.2(3)	C(4)–C(5)–C(6)	121.2(5)	C(8)–C(9)–C(4)	119.4(4)
C(1)#1–C(2)–C(1)	113.0(6)	C(7)–C(6)–C(5)	120.0(5)	C(11)–C(10)–C(9)	122.2(5)
N(1)–C(3)–C(4)	122.0(4)	C(6)–C(7)–C(8)	121.6(5)	C(10)–C(11)–C(12)	120.3(5)
C(5)–C(4)–C(9)	118.5(4)	C(7)–C(8)–C(9)	119.2(5)	C(13)–C(12)–C(11)	119.6(5)
C(5)–C(4)–C(3)	119.8(4)	C(7)–C(8)–C(13)	121.0(5)	C(12)–C(13)–C(8)	120.9(5)
C(9)–C(4)–C(3)	121.6(4)	C(9)–C(8)–C(13)	119.8(5)		

Symmetry transformations used to generate equivalent atoms: #1 $-x+1$, y, $-z+1$.

atoms (O(3), O(4), O(3)#, O(4)#) from two [NiL] chelates, and both oxygen atoms (O(6), O(6)#) from the ligating acetate ions, μO–C–O, also with octahedral geometry. The trinuclear structure is stabilized by two μ-acetato ligands.

The interatomic distances of Ni(1)–Ni(2) (3.083(6) Å) is significantly longer than all the Ni–O and Ni–N bonds in the cluster (table 3) and considerably shorter

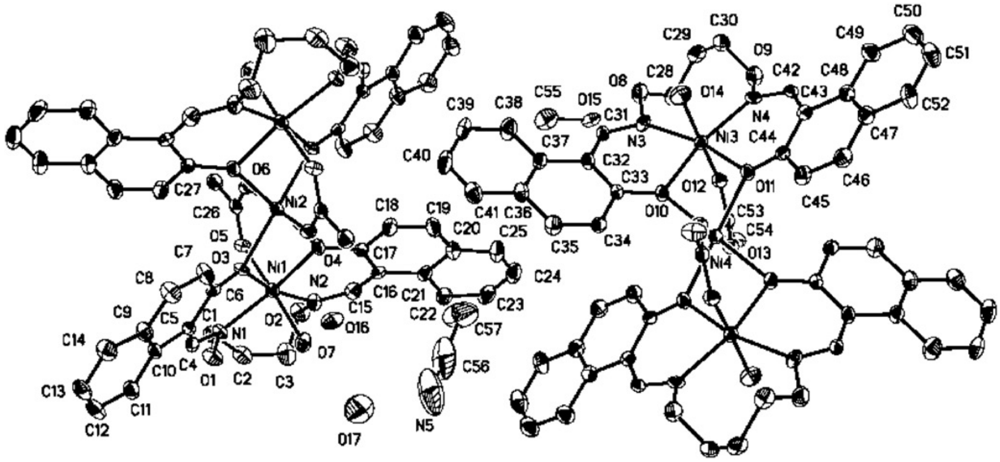

Figure 4. The structure of **1** with the atom numbering. Displacement ellipsoids for non-H atoms are drawn at the 30% probability level. Each nickel has octahedral geometry.

Table 3. Selected bond distances (Å) and angles (°) for **1**.

Ni(1)–O(3)	2.008(5)	Ni(2)–O(4)	2.069(5)	Ni(3)–N(3)	2.087(6)
Ni(1)–O(5)	2.031(6)	Ni(2)–O(4)#1	2.069(5)	Ni(3)–O(14)	2.112(6)
Ni(1)–O(4)	2.032(5)	Ni(2)–O(3)#1	2.100(5)	Ni(4)–O(13)	2.050(6)
Ni(1)–N(1)	2.049(6)	Ni(2)–O(3)	2.100(5)	Ni(4)–O(13)#2	2.050(6)
Ni(1)–N(2)	2.083(7)	Ni(3)–O(11)	2.010(5)	Ni(4)–O(11)	2.067(5)
Ni(1)–O(7)	2.099(6)	Ni(3)–O(10)	2.012(5)	Ni(4)–O(11)#2	2.067(5)
Ni(2)–O(6)#1	2.045(6)	Ni(3)–O(12)	2.028(5)	Ni(4)–O(10)#2	2.084(5)
Ni(2)–O(6)	2.045(6)	Ni(3)–N(4)	2.072(6)	Ni(4)–O(10)	2.084(5)
O(3)–Ni(1)–O(5)	91.8(2)	O(4)–Ni(2)–O(4)#1	180.0(2)	O(11)–Ni(3)–O(14)	90.9(2)
O(3)–Ni(1)–O(4)	80.2(2)	O(6)#1–Ni(2)–O(3)	89.6(2)	O(10)–Ni(3)–O(14)	92.6(2)
O(5)–Ni(1)–O(4)	92.4(2)	O(6)–Ni(2)–O(3)	90.4(2)	O(12)–Ni(3)–O(14)	175.1(2)
O(3)–Ni(1)–N(1)	85.7(2)	O(4)–Ni(2)–O(3)	77.3(2)	N(4)–Ni(3)–O(14)	87.4(3)
O(5)–Ni(1)–N(1)	90.5(2)	O(4)#1–Ni(2)–O(3)	102.7(2)	N(3)–Ni(3)–O(14)	87.1(3)
O(4)–Ni(1)–N(1)	165.7(2)	O(6)#1–Ni(2)–O(3)#1	90.4(2)	O(13)–Ni(4)–O(13)#2	180.0(3)
O(3)–Ni(1)–N(2)	166.9(2)	O(6)–Ni(2)–O(3)#1	89.6(2)	O(13)–Ni(4)–O(11)#2	90.0(2)
O(5)–Ni(1)–N(2)	89.0(3)	O(4)–Ni(2)–O(3)#1	102.7(2)	O(13)#2–Ni(4)–O(11)#2	90.0(2)
O(4)–Ni(1)–N(2)	86.7(2)	O(4)#1–Ni(2)–O(3)#1	77.3(2)	O(13)–Ni(4)–O(11)	90.0(2)
N(1)–Ni(1)–N(2)	107.3(3)	O(3)#1–Ni(2)–O(3)	180.000(2)	O(13)#2–Ni(4)–O(11)	90.0(2)
O(3)–Ni(1)–O(7)	91.1(2)	O(11)–Ni(3)–O(10)	80.1(2)	O(11)–Ni(4)–O(11)#2	180.000(1)
O(5)–Ni(1)–O(7)	175.7(2)	O(11)–Ni(3)–O(12)	92.8(2)	O(13)–Ni(4)–O(10)#2	90.6(2)
O(4)–Ni(1)–O(7)	91.1(2)	O(10)–Ni(3)–O(12)	91.2(2)	O(13)#2–Ni(4)–O(10)#2	89.4(2)
N(1)–Ni(1)–O(7)	86.6(3)	O(11)–Ni(3)–N(4)	85.1(2)	O(11)–Ni(4)–O(10)#2	102.8(2)
N(2)–Ni(1)–O(7)	88.9(3)	O(10)–Ni(3)–N(4)	165.3(2)	O(11)#2–Ni(4)–O(10)#2	77.2(2)
O(6)#1–Ni(2)–O(6)	180.000(2)	O(12)–Ni(3)–N(4)	89.7(2)	O(13)–Ni(4)–O(10)	89.4(2)
O(6)#1–Ni(2)–O(4)	90.3(2)	O(11)–Ni(3)–N(3)	165.3(3)	O(13)#2–Ni(4)–O(10)	90.6(2)
O(6)–Ni(2)–O(4)	89.7(2)	O(10)–Ni(3)–N(3)	85.4(2)	O(11)–Ni(4)–O(10)	77.2(2)
O(6)#1–Ni(2)–O(4)#1	89.7(2)	O(12)–Ni(3)–N(3)	90.1(2)	O(11)#2–Ni(4)–O(10)	102.8(2)
O(6)–Ni(2)–O(4)#1	90.3(2)	N(4)–Ni(3)–N(3)	109.3(3)	O(10)#2–Ni(4)–O(10)	180.0(3)

Symmetry transformations used to generate equivalent atoms: #1: $-x+1, -y+2, -z+1$; #2: $-x+2, -y+1, -z+1$.

than those of previously reported salen-type chelates, {[Ni(H_4Salpr)(H_2O)]$_2$(OAc)$_2$Ni} [16], {[Ni(Salpr)(NC_5H_5)]$_2$(OAc)$_2$Ni} [16], {[Ni(Salpr)(NC_5H_5)]$_2$(OAc)$_2$Ni} [17], {[Ni(Salpr)(DMF)]$_2$(NO_3)$_2$Ni} [18], {[Ni(Salpr)(DMSO)]$_2$(OAc)$_2$Ni} [19] and {[Ni(Salpr)(DMF)]$_2$(OAc)$_2$Ni} [20], indicating a stronger intermetal interaction similar

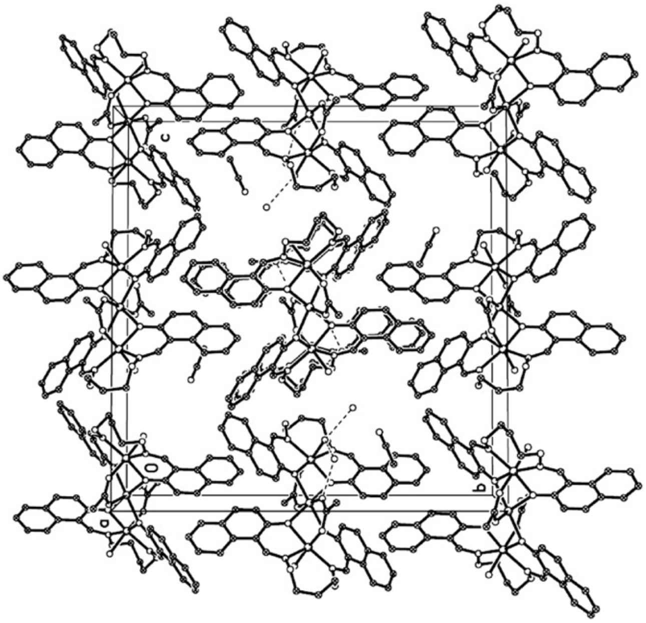

Figure 5. Packing diagram of **1** along *c*-axis. H atoms are omitted for clarity.

Table 4. Intramolecular H-bond (Å, °) details for **1**.

D–H ⋯ A	d(D–H)	d(H ⋯ A)	∠DHA	d(D ⋯ A)
O7–H57 ⋯ O16	0.850	1.920	151.20	2.696
O7–H58 ⋯ O17	0.850	2.111	137.05	2.794
O14–H59 ⋯ O15^{i}	0.850	1.767	164.50	2.596
O15–H15 ⋯ O13^{ii}	0.820	2.037	141.97	2.730
O16–H63 ⋯ O2^{i}	0.850	2.316	141.48	3.028
O16–H64 ⋯ O6^{iii}	0.850	1.934	150.76	2.708
O17–H65 ⋯ O8^{iv}	0.850	2.131	166.89	2.965
O17–H66 ⋯ O7	0.850	2.011	152.90	2.794

Symmetry codes: (i) $x+1$, y, z; (ii) $-x+1$, $-y+1$, $-z+1$; (iii) $-x+1$, $-y+2$, $-z+1$; (iv) x, $-y+3/2$, $z+1/2$.

to our previously reported bisoxime octanuclear analogues, $[Zn_8L_4(H_2O)_3]\cdot 4.5H_2O$ and $[Co_8L_4(H_2O)_2X]\cdot 2H_2O\cdot 1.5CHCl_3\cdot 0.5$hexane ($X = H_2O$ or EtOH) [13].

The unit cell packing of **1**, illustrated in figure 5, shows the space formed by packing of cluster molecules. Hydrogen bonding interactions (table 4), μ-acetato and μ-phenoxo bridging, play a critical role in assembly, stability and crystallization of the cluster.

Further investigation on the synthesis and the structure of complexes with copper, cobalt, zinc, iron and manganese is now in progress.

Supplementary data

Further details of the crystal structure investigation(s) may be obtained from the Cambridge Crystallographic Data Centre, Postal Address: CCDC, 12 Union Road, Cambridge CB2 1EZ, UK. Telephone: (44) 01223 762910; Facsimile: (44) 01223 336033;

Email: deposit@ccdc.cam.ac.uk, on quoting the depository number CCDC Nos: 626923 for H_2L and 629217 for **1**.

Acknowledgements

This work was supported by the Foundation of the Education Department of Gansu Province (No. 0604-01) and the 'Qing Lan' Talent Engineering Funds of Lanzhou Jiaotong University (QL-03-01A), which are gratefully acknowledged.

References

[1] P.G. Cozzi. *Chem. Soc. Rev.*, **33**, 410 (2004).
[2] R. Ziessel. *Coord. Chem. Rev.*, **216**, 195 (2001).
[3] M.R. Bermejo, A. Castineiras, J.C. Garcia-Monteagudo, M. Rey, A. Sousa, M. Watkinson, C.A. McAuliffe, R.G. Pritchard, R.L. Beddose. *J. Chem. Soc.*, **2935** (1996).
[4] M. Watkinson, M. Fondo, M.R. Bermejo, A. Sousa, C.A. McAuliffe, R.G. Pritchard, N. Jaiboon, N. Aurangzeb, M. Naeem. *J. Chem. Soc.*, 31 (1999).
[5] M. Ramesh, K.B. Chandrasekar, K.H. Reddy. *Indian J. Chem.*, **39A,**, 1337 (2000).
[6] E.G. Samsel, K. Srinivasan, J.K. Kochi. *J. Am. Chem. Soc.*, **107**, 7606 (1985).
[7] E.N. Jacobsen, W. Zhang, A.R. Muci, J.R. Ecker, L. Deng. *J. Am. Chem. Soc.*, **113**, 7063 (1991).
[8] N.S. Venkataramanan, G. Kuppuraj, S. Rajagopal. *Coord. Chem. Rev.*, **249**, 1249 (2005).
[9] S. Akine, T. Nabeshima. *Inorg. Chem.*, **44**, 1205 (2005).
[10] C.M. Che, J.S. Huang. *Coord. Chem. Rev.*, **242**, 97 (2003).
[11] E. Dunach, A.P. Esteves, M.J. Medeiros, D. Pletcher, S. Olivero. *J. Electroanal. Chem.*, **39**, 566 (2004).
[12] S. Akine, T. Taniguchi, W.K. Dong, T. Nabeshima. *J. Org. Chem.*, **70**, 1704 (2005).
[13] S. Akine, W.K. Dong, T. Nabeshima. *Inorg. Chem.*, **45**, 4677 (2006).
[14] W.K. Dong, J.H. Feng. *Acta Crystallogr.*, **E62**, o3577 (2006).
[15] W.K. Dong, R.D. Yang. *Synth. React. Inorg. Met.-Org. Chem.*, **29**, 1631 (1999).
[16] J. Reglinski, M.K. Taylor, A.R. Kennedy. *Inorg. Chem. Commun.*, **9**, 736 (2006).
[17] J. Reglinski, S. Morris, D.E. Stevenson. *Polyhedron*, **21**, 2167 (2002).
[18] O. Atakol, C. Arici, M.N. Tahir, R. Kurtaran, D. Ulku. *Anal. Sci.*, **13**, 933 (1999).
[19] D. Ulku, F. Ercan, O. Atakol, F.N. Dincer. *Acta Crystallgr.*, **C53**, 1056 (1997).
[20] A. Elmali, V. Elerman, I. Svoboda, H. Feuss, K. Griesar, W. Haase. *Z. Naturforsch.*, **B51**, 665 (1995).